Optimal Arrangement of Current Leads to Minimize Electromagnetic Force

J. H. Lee, J. B. Song, K. L. Kim, K. J. Kim, M. J. Kim, H. M. Chang, and H. G. Lee

***Abstract*—An electric current produces a magnetic field around a current lead, which attracts or repels other current leads. The electromagnetic forces interacting between current leads show different tendencies according to the arrangement of the current leads on the top flange of the cryostat and the distances between them. In the case of high-current electric power devices or high-field magnets, the optimal arrangement of the current leads that can minimize the electromagnetic force acting on them is one of the safety issues to be considered. In this paper, the electromagnetic forces exerted on current leads were examined theoretically. The results were confirmed by measuring the strain variations of the current leads using a strain gauge to determine the influence of the electrical and geometrical parameters. From these results, the optimal arrangement method is discussed with three pairs of current leads particularly for high-current electric power devices or high-field magnet applications.**

***Index Terms*—Current lead, electromagnetic force, high-current electrical power device, high-field magnet application.**

I. Introduction

ELECTROMAGNETIC forces interacting between current leads are generated when an electrical current flows through them. In the case of high-current electric power devices or high-field magnets, the electromagnetic forces acting on the current leads are considerable so that a careless configuration of the current leads can cause some damage to the system, such as mechanical deformation and electrical short circuits due to bending stress [1]. In practice, a fault current, which is ~20 times its rated current, occurs in the fault-mode of a superconducting fault current limiter (SFCL). For a large fusion machine, such as the International Thermonuclear Experimental Reactor (ITER), the magnetic field in the central solenoid is up to 13 T and the operating current is approximately 40 kA [2]–[4]. Therefore, the electromagnetic forces upon the current leads should be considered when they are installed on the top flange of a cryostat. Theoretically, the electromagnetic forces show different tendencies according to the arrangement of the current leads and the distances between them. Therefore, an optimal arrangement is required to minimize the electromagnetic forces on the current leads.

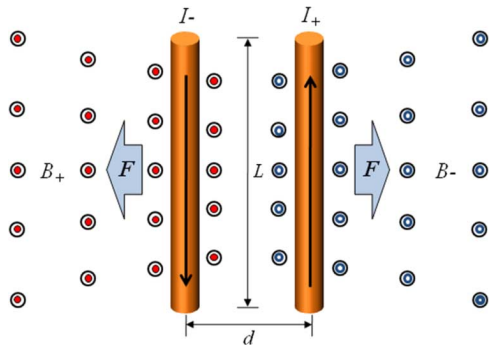

Fig. 1. Electromagnetic force between two long straight parallel current leads.

In this study, the electromagnetic forces between current leads were calculated theoretically, and the results were confirmed by measuring the strain variations in the current leads under the electromagnetic force using a strain gauge. This paper discusses the influence of the electrical and geometrical parameters on the mechanical stability of the current leads, and finally suggests an optimal arrangement with three pairs of current leads for high-current electric power devices or high-field magnet applications.

II. Theory of Electromagnetic Forces Acting on Current Leads

A. Electromagnetic Forces Acting on One Pair of Current Leads

Consider two long straight parallel current leads separated by a distance d carrying currents I_+ and I_-, and examine the case where the two currents are in opposite directions, as indicated in Fig. 1. One lead $(+)$ will experience a magnetic field $(\vec{\mathbf{B}}_-)$ from another lead $(-)$ given by (1), and will experience a repulsive force given by (2)

$$|\vec{\mathbf{B}}_-| = B_- = \frac{\mu_0 I_-}{2\pi d} \tag{1}$$

$$|\vec{\mathbf{F}}_+| = |I_+ \vec{\mathbf{L}}_+ \times \vec{\mathbf{B}}_-| = \frac{\mu_0 I_-}{2\pi d} I_+ L_+. \tag{2}$$

Where, $\vec{\mathbf{L}}_+$ is a vector whose magnitude is the length of the lead $(+)$, L_+, and whose direction is along the lead $(+)$ aligned

Manuscript received October 20, 2009. First published March 01, 2010; current version published May 28, 2010. This work was supported by the Korea Science and Engineering Foundation (KOSEF) Grant funded by the Korea Government (MEST 2009-0085369), and by a Grant from the Center for Applied Superconductivity Technology of the 21st Century Frontier R&D Program funded by the Ministry of Education, Science and Technology, Korea.

J. H. Lee, J. B. Song, K. L. Kim, K. J. Kim, and H. G. Lee are with the Department of Materials Science and Engineering, Korea University, Seoul, Korea (e-mail: haigunlee@korea.ac.kr).

M. J. Kim and H. M. Chang are with the Department of Mechanical and System Design Engineering, Hong Ik University, Seoul, Korea.

Color versions of one or more of the figures in this paper are available online at http://ieeexplore.ieee.org.

Digital Object Identifier 10.1109/TASC.2010.2040956

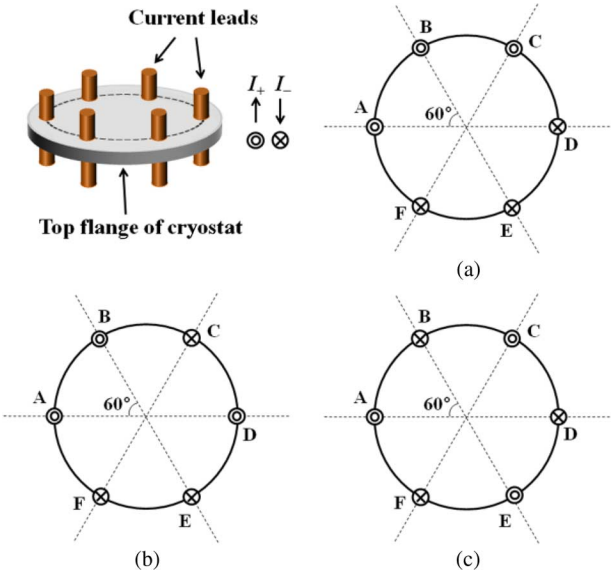

Fig. 2. Arrangement methods for three pairs of current leads: (a) Arrangement 1, (b) Arrangement 2, and (c) Arrangement 3.

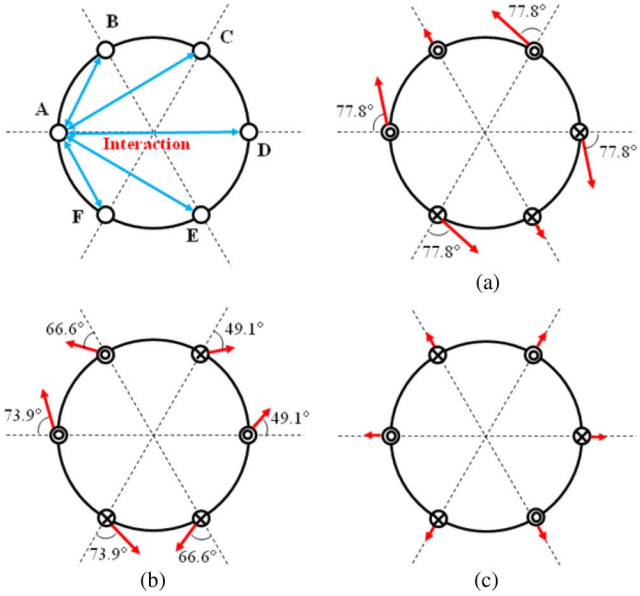

Fig. 3. Directions of the electromagnetic forces on each current lead with respect to the arrangement methods: (a) Arrangement 1, (b) Arrangement 2, and (c) Arrangement 3.

in the direction of current flow, $\vec{\mathbf{F}}_+$ is the electromagnetic force upon the lead $(+)$, and μ_0 is the magnetic permeability of free space $(4\pi \times 10^{-7}\,\mathrm{H/m})$. Assuming that the same current flows through both leads $(I = I_+ = I_-)$, the magnitude of the electromagnetic force per unit length acting on lead $(+)$, f_+, can be expressed by the following equation:

$$f_+ = \frac{|\vec{\mathbf{F}}_+|}{L_+} = \frac{\mu_0}{2\pi}\frac{I^2}{d} = 2 \times 10^{-7} \times \frac{I^2}{d}. \tag{3}$$

B. Arrangement Methods of Three Pairs of Current Leads

In the case of a complicated high-current electric power device, where many current leads are required, both electric and magnetic interactions between the current leads are more complicated and their effects on the electromagnetic forces could be much stronger according to the arrangement and distances between them. Therefore, geometrical parameters should be considered carefully before installing them on the top flange of a cryostat. First of all, it is recommended to arrange the current leads along the line of the circumference with radius R to maximize the distances because the electromagnetic force is inversely proportional to the distance between current leads. In addition, the direction and magnitude of the electromagnetic force acting on a current lead are determined by a combination of the current-flowing directions of the other current leads so that an appropriate configuration is required.

With three pairs of current leads, there are three possible arrangements except for symmetrical ones, as shown in Fig. 2. In all cases, the net electromagnetic forces on current lead A, $\vec{\mathbf{F}}_{Total,A}$, are given by vector summation of all forces acting on lead A by the other leads B, C, D, E, and F according to the following equations:

$$\vec{\mathbf{F}}_{Total,A} = \vec{\mathbf{F}}_{BA} + \vec{\mathbf{F}}_{CA} + \vec{\mathbf{F}}_{DA} + \vec{\mathbf{F}}_{EA} + \vec{\mathbf{F}}_{FA} \tag{4}$$

$$f_{Total,A} = \frac{|\vec{\mathbf{F}}_{Total,A}|}{L_A}$$

$$= \frac{|\vec{\mathbf{F}}_{BA} + \vec{\mathbf{F}}_{CA} + \vec{\mathbf{F}}_{DA} + \vec{\mathbf{F}}_{EA} + \vec{\mathbf{F}}_{FA}|}{L_A}. \tag{5}$$

Where, $\vec{\mathbf{F}}_{BA}$, $\vec{\mathbf{F}}_{CA}$, $\vec{\mathbf{F}}_{DA}$, $\vec{\mathbf{F}}_{EA}$ and $\vec{\mathbf{F}}_{FA}$ are the forces acting upon current lead A by the other leads B, C, D, E and F, respectively, L_A is the active length of lead A, and $f_{Total,A}$ is the total electromagnetic force per length acting on lead A.

Fig. 3 shows a schematic diagram of the directions of the electromagnetic forces on each current lead with respect to the three possible arrangements. In the case of Arrangement 1, as shown in Fig. 3(a), the orientations of current flowing through leads A, B and C are opposite to those of leads D, E and F. Therefore, attractive and repulsive forces are symmetrical with respect to an imaginary straight line passing through two center points: one between leads A and F, and another between leads C and D. The electromagnetic forces on leads A, C, D and F are the same and their values are 4.73 times as strong as those of leads B and E (see Fig. 4). As expected, the distribution of electromagnetic forces is unbalanced and concentrated in two directions, which are headed for an imaginary straight line through leads B or E from the center.

In the case of Arrangement 2, each lead has a random sign: current leads A$(+)$, B$(+)$, C$(-)$, D$(+)$, E$(-)$ and F$(-)$, are located randomly, as shown in Fig. 3(b). In this arrangement, the electromagnetic forces on each current lead are unbalanced and oriented randomly.

In the case of Arrangement 3, as shown in Fig. 3(c), leads A, B, C, D, E and F has a sign in order of $(+)$, $(-)$, $(+)$, $(-)$, $(+)$, and $(-)$, respectively. In contrast to Arrangements 1 and 2, the attractive and repulsive forces have six-fold rotation symmetry. Because of this symmetry, the net force on each current lead is always directed outward from the center, i.e. a repulsive force. In addition, the electromagnetic forces on all current leads are equal and their values are the smallest among the three arrangements.

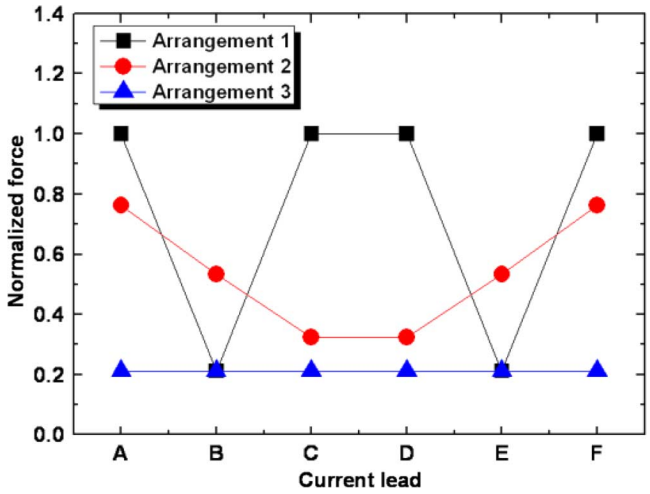

Fig. 4. The normalized electromagnetic forces on all current leads in each arrangement.

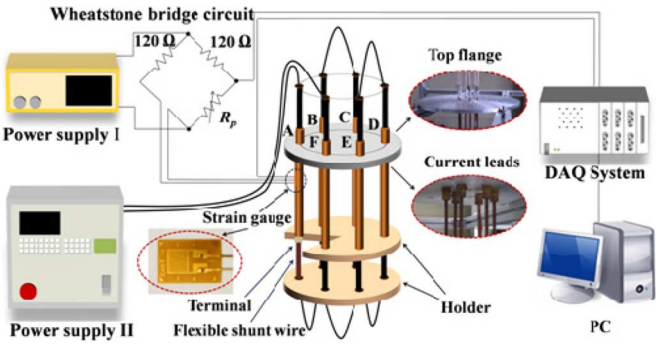

Fig. 5. Schematic diagram of the experimental set-up.

TABLE I
PARAMETERS OF THE CURRENT LED, TERMINAL, SHUNT WIRE, AND STRAIN GAUGE

Parameters	Values
Current lead (copper)	
Diameter, D	0.4 cm
Total active length	50 cm
Length from the strain gauge to the edge, L	44 cm
Young's modulus, E	110 GPa
Terminal (copper)	
Overall Length, L'	1.5 cm
Shunt wire (copper)	
Overall Length, L''	15 cm
Strain gauge	
Dimension	0.3 cm × 0.5 cm
Gauge factor, GF	2.1
Nominal resistance, R_G	120 Ω
Self temperature compensation (STC)	16
Excitation voltage, V_{EX}	5 V

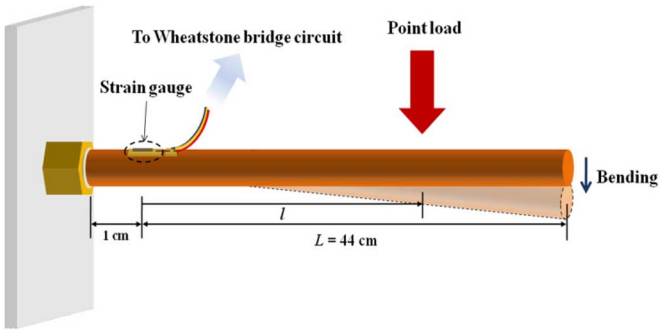

Fig. 6. Schematic diagram of a point load on a horizontal current lead.

Fig. 4 shows the normalized forces acting on each current lead according to theory (5) in each arrangement. Based on these simulations, Arrangement 3 (same order coordination) is the best arrangement method to reduce the active magnetic forces between current leads.

III. EXPERIMENTAL

Fig. 5 shows a schematic diagram of the experimental set-up used in this study. A copper (>99.9%) rod, 50 cm in length and 2 mm in radius, was chosen as a current lead because of its high thermal/electrical conductivity and ductility. The current leads were fixed to the top flange with straights and electrical tape pasted with an epoxy resin was used for electrical insulation of the current leads from the straights and top flange. For current injection to the current leads, the ends of the lead terminals were shunted with flexible copper wire.

In order to obtain the electromagnetic forces exerted on the current leads, the strain variations were measured from the current lead with the strain gauge (AP-16-S10S-120-EL), whose self temperature compensation (STC) number, gauge factor (GF) and nominal resistance (R_G) were 16, 2.1 and 120 Ω, respectively. The Wheatstone bridge circuit illustrated in Fig. 5 consists of four resistive arms. One of them is the strain gauge (quarter-bridge configuration) with an excitation voltage, V_{EX}, that is applied across the bridge. A potential meter (R_P) was used to initially balance the bridge in order to generate a zero output voltage (V_o) when no strain is applied. The output voltage from this circuit was acquired using a data acquisition (DAQ) system. From the output voltage, the strain (ε^{Exp}) generated by the electromagnetic force acting on each current lead was obtained using the following equation [5]:

$$\varepsilon^{Exp} = \frac{4}{GF} \times \frac{V_o}{V_{EX}}. \tag{6}$$

Table I lists the property data and parameters of the current lead, terminal, shunt wire, and strain gauge used in this study.

IV. RESULTS AND DISCUSSION

A. Measurements Techniques for Electromagnetic Forces

Fig. 6 shows a schematic diagram of a point load on a horizontal current lead. In general, the degree of bending of a current lead is determined by the load and load point. The strain caused by bending stress due to the point load (ε_P^{Com}) was calculated as follows:

$$\varepsilon_P^{Com} = \frac{M}{ZE}. \tag{7}$$

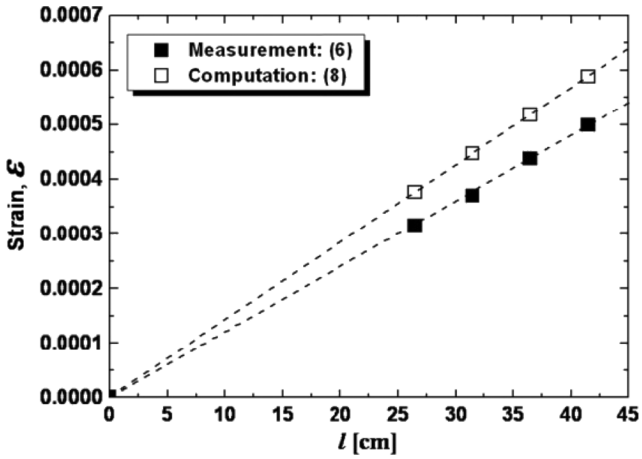

Fig. 7. Strain vs. l plots ($W = 0.98$ N) obtained from measurement (6) and computation (8).

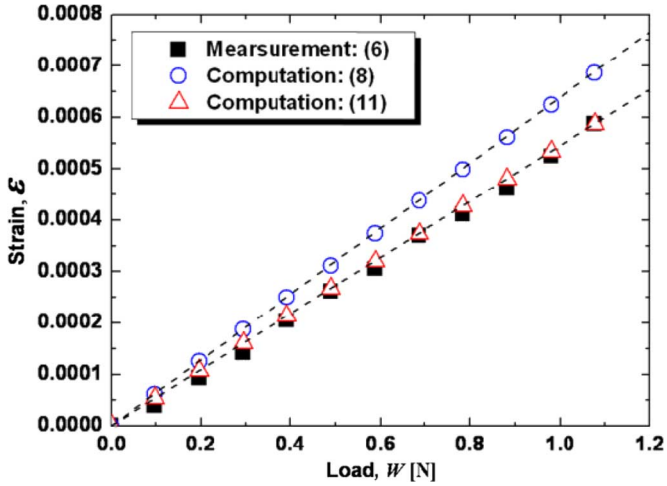

Fig. 8. Strain vs. W plots ($l = L = 44$ cm) obtained from the measurement (6) and computations (8), (11).

Where, M is bending moment, Z is the sectional modulus and E is the Young's modulus of the current lead. In a right circular cylinder-like object, M and Z are Wl (W: a point load, l: an arbitrary distance from the strain gauge to the load point) and $\pi D^3/32$ (D: diameter of cross section of the current lead), respectively [6]. The strain equation can be obtained as a function of l by inserting these two expressions into (7)

$$\varepsilon_P^{Com}(l) = \frac{32Wl}{\pi D^3 E}. \tag{8}$$

On the other hand, a homogeneously distributed force, such as an electromagnetic force, is exerted equally over all parts of the current lead. Hence, the strain should be obtained by the summation of all forces acting on each infinitesimal part of the lead. Assuming that the current lead experiences a homogeneously distributed force ($f = dW/dl$), the net strain (ε_H^{Com}) can be obtained by integrating (8) with respect to l

$$\varepsilon_H^{Com} = \int_0^L \frac{32fl}{\pi D^3 E} dl = \frac{16fL^2}{\pi D^3 E}. \tag{9}$$

Where, L is the distance from the strain gauge to an edge of the current lead. In addition, W at $l = L$ can be converted to a homogeneously distributed force by equating (8) and (9)

$$f = \frac{2}{L}W. \tag{10}$$

In order to verify the effects of W and l on the strain, the strain was measured with various W at different l on the horizontal copper lead. Fig. 7 shows the strain vs. l plots at $W = 0.98$ N, obtained by the measurement (6) and computation (8). Both ε^{Exp} (6) and ε_P^{Com} (8) increased linearly with increasing l and the ratio of the slopes of these two lines was 1.13 (i.e., 13% discrepancy).

In order to solve the discrepancy between the measurement and computation, (11) was derived by equating (6) and (8) or (9) with the correction factor

$$\varepsilon^{Exp} = \alpha\varepsilon_P^{Com}(l = L) = \alpha\frac{32WL}{\pi D^3 E} = \alpha\varepsilon_H^{Com} = \alpha\frac{16fL^2}{\pi D^3 E}. \tag{11}$$

Where, α is the correction factor, and was obtained by rearranging (11) as follows:

$$\alpha = \frac{\pi D^3 E}{32WL}\varepsilon^{Exp} \text{ or } \alpha = \frac{\pi D^3 E}{16fL^2}\varepsilon^{Exp}. \tag{12}$$

Using (12), α was found to be 0.855.

Fig. 8 shows the strain vs. W plots ($l = L = 44$ cm) obtained from the measurement (6) and computations (8), (11). The measured values (solid squares) obtained from (6) are similar to those (open triangles) calculated from (11), as expected, while there was 13% deviation between the measurement (6) and computation by (8).

Combining (6) and (12), the electromagnetic force per length (f^{Exp}) was obtained simply using the following relationship:

$$f^{Exp} = \frac{\pi D^3 E}{16\alpha L^2}\varepsilon^{Exp}. \tag{13}$$

In the case of current injection to the leads, a shunt wire needs to be connected between the terminals of the leads. An extra strain effect will also be considered because they also experience an electromagnetic force when a current flows through the current leads. Therefore, the extra strain ($\varepsilon_{extra}^{Com}$) from the terminal ($\varepsilon_{ter}^{Com}$) and shunt wire ($\varepsilon_{wire}^{Com}$) should be added to (11). Equation (11) can then be rearranged as follows:

$$\varepsilon^{Exp} = \alpha\left(\frac{16L^2}{\pi D^3 E}f + \varepsilon_{extra}^{Com}\right) \tag{14}$$

where

$$\varepsilon_{extra}^{Com} = \varepsilon_{ter}^{Com} + \varepsilon_{wire}^{Com}. \tag{15}$$

Since the terminal is stiff and attached tightly to the edge of the lead, it can be regarded as being a part of the current lead, and its influence on the strain could be evaluated by integrating (9) with respect l in the range of L and $L + L'$

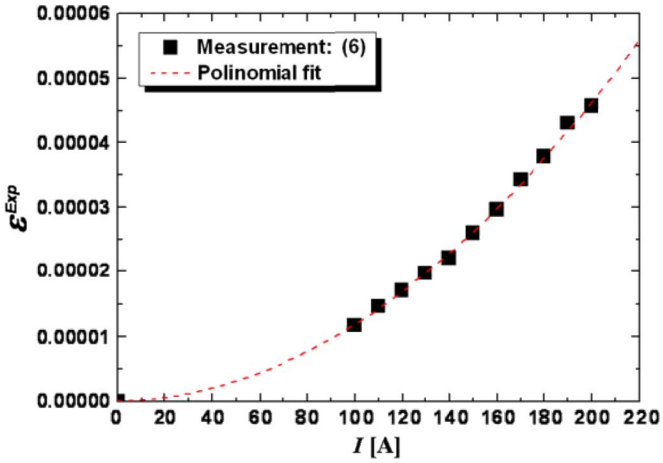

Fig. 9. Strain variations with respect to I in a single pair of the current leads ($d = 3$ cm, and $I = 100 \sim 200$ A), obtained by measurement (6).

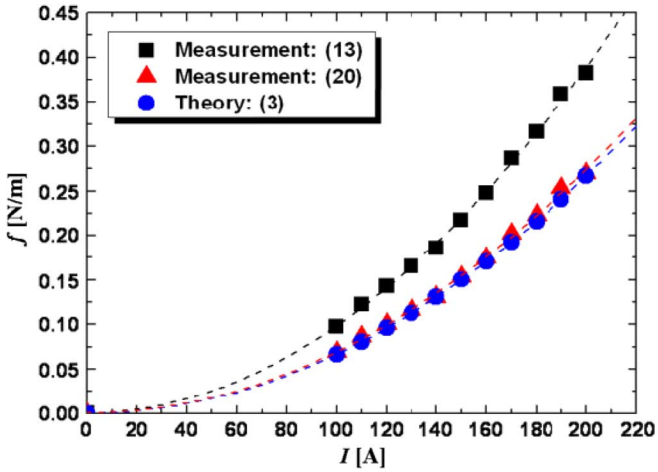

Fig. 10. Electromagnetic force per length (f) vs. I plots in one pair of current leads ($d = 3$ cm, and $I = 100 \sim 200$ A), obtained by theory (3) and measurements (13), (20).

$$\varepsilon_{ter}^{Com} = \int_{L}^{L+L'} \frac{32fl}{\pi D^3 E} dl = \frac{16\left[(L+L')^2 - L^2\right]}{\pi D^3 E} f. \quad (16)$$

However, for the shunt wire, the effective force ($\mathrm{f}' = \mathrm{dW/dl}$) acting on the strain in l ranging from $L + L'$ to $L + L' + L''$ (L'': length of the shunt wire) was not constant but a function of l. Assuming that this force decreases linearly as l approaches from $L + L'$ to $L + L' + L''$, it can be expressed as follows:

$$f'(l) = f\frac{(L+L'+L'') - l}{L''}. \quad (17)$$

By inserting (17) into (9), we obtain

$$\begin{aligned}\varepsilon_{wire}^{Com} &= \int_{L+L'}^{L+L'+L''} \frac{32f'l}{\pi D^3 E} dl \\ &= \int_{L+L'}^{L+L'+L''} \frac{32fl}{\pi D^3 E} \frac{(L+L'+L'') - l}{L''} dl. \end{aligned} \quad (18)$$

The following can be derived by integrating (18) with respect to l in the range of $L + L'$ and $L + L' + L''$:

$$\varepsilon_{wire}^{Com} = \frac{4(L+L')^2 + 7(L+L')L'' + 2L''^2}{6} \cdot \frac{32}{\pi D^3 E} f. \quad (19)$$

From (14), (16) and (19), we have an expression for the modified electromagnetic force, f_{mdf}^{Exp}, as follows:

$$f_{\mathrm{m}df}^{Exp} = \frac{\pi D^3 E}{16\alpha} \cdot \frac{3\varepsilon^{Exp}}{7(L+L')^2 + 7(L+L')L'' + 2L''^2}. \quad (20)$$

B. One Pair of Current Leads

One pair of current leads was used to confirm the feasibility of this measurement technique. Fig. 9 shows the strain variations with respect to the applied current (I) in the range of 100 and 200 A ($d = 3$ cm). As predicted by theory, ε^{Exp} is proportional to the square of I. With these ε^{Exp}, the electromagnetic forces per length (f) acting on the current leads were also obtained. Fig. 10 shows the f vs. I plots obtained by theory (3) and measurements (13), (20). The solid squares represent f^{Exp} obtained by (13), which were 34% over the solid circles (f) calculated from (3) while the solid triangles (f_{mdf}^{Exp}) obtained from (20) were similar to the values (solid circles) determined from theory (3).

C. Three Pairs of Current Leads

As mentioned earlier, in the case of three pairs of current leads, there are three possible arrangements. Among them, arrangement 3 was found to be the optimal method to minimize f acting on the current leads. The measurements were carried out to verify the theoretical results (5) with the experiments according to the arrangement methods.

Fig. 11 shows f with respect to the arrangement methods in three pairs of current leads ($d = 3$ cm, and $I = 200$ A), obtained by theory (5) and measurement (20). As expected, f_{mdf}^{Exp} measured by (20) is almost equal to f computed by (5).

Fig. 12 shows the magnitudes and directions of f exerted on each current lead in the three different arrangement methods ($d = 3$ cm, and $I = 200$ A). The theoretical values are also shown in the parentheses. Agreement between the measurement and theory was quite good. The values of f acting on all leads in Arrangement 3 showed the lowest values, which were 20 to 25% of the values obtained from Arrangements 1 and 2. Among the three arrangements, Arrangement 3 was found to be the optimal arrangement for minimizing the active electromagnetic forces upon the current leads. This means that the arrangement method of the current leads is an important factor for the stability of the system, particularly in the case of high-current electric power devices or high-field magnet applications.

V. Conclusion

In this study, the electromagnetic forces exerted on current leads placed in three different arrangements were examined theoretically. The results were confirmed by measuring the strain

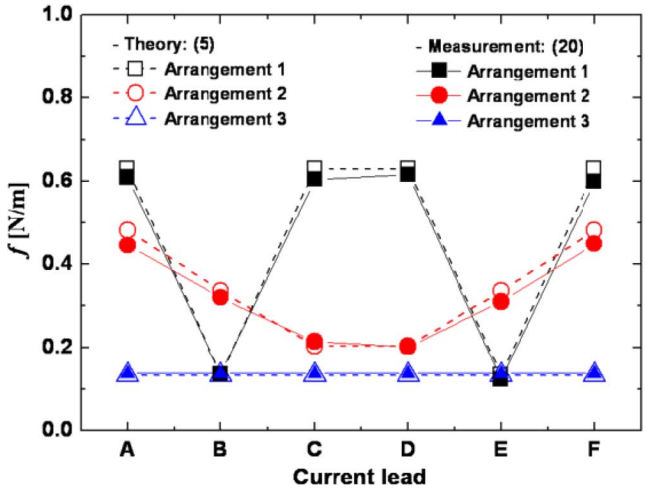

Fig. 11. The f in three pairs of the current leads, obtained by theory (5) and measurement (20) ($d = 3$ cm, and $I = 200$ A).

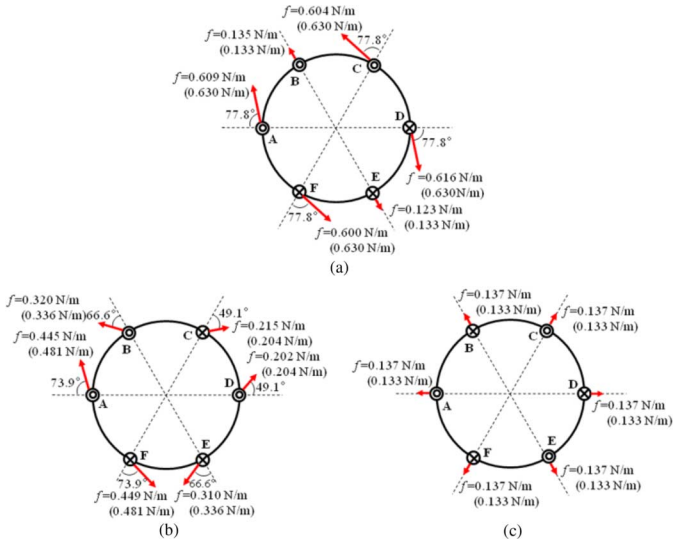

Fig. 12. The magnitudes and directions of f acting on each current lead ($d = 3$ cm, and $I = 200$ A), obtained by measurement and computation (in parenthesis): (a) Arrangement 1, (b) Arrangement 2, and (c) Arrangement 3.

variations in the current leads with a strain gauge to determine the influence of the electrical and geometrical parameters. The current leads were along the line of the circumference to maximize the distance between them and the current-flowing directions of each lead with respect to the arrangement methods were as follows: A(+), B(+), C(+), D(−), E(−), and F(−) in Arrangement 1, A(+), B(+), C(−), D(+), E(−), and F(−) in Arrangement 2, and A(+), B(−), C(+), D(−), E(+), and F(−) in Arrangement 3. The electromagnetic forces acting on all the leads in Arrangement 3 showed the lowest values, which were 20 to 25% lower than those in Arrangements 1 and 2. The values of these forces were only 22% of those on leads A, C, D, and F in Arrangement 1. This suggests that Arrangement 3 is the optimal arrangement for three pairs of current leads. In the case of high-current electric power devices or high-field magnets, where the electromagnetic forces acting on the current leads are considerably large, it is essential that the current leads be arranged appropriately for the stability of the system.

REFERENCES

[1] J. H. Kim, J. B. Song, S. J. Hwang, K. L. Kim, H. M. Kim, H.-R. Kim, O. B. Hyun, T. K. Ko, and H. G. Lee, "Optimal arrangement of current leads for 24 kV class SFCL to minimize electromagnetic force," *J. Kor. Inst. Appl. Supercond. Cryogenics*, vol. 9, pp. 62–66, 2007.

[2] Y. Nunoya, T. Isono, and K. Okuno, "Experimental investigation on the effect of transverse electromagnetic force on the V-T curve of the CIC conductor," *IEEE Trans. Appl. Supercond.*, vol. 14, pp. 1468–1472, 2004.

[3] S. R. Lee, J. Y. Park, J. Y. Yoon, B. J. Lee, and B. M. Yang, "Specifications of 22.9 kV HTS cables and FCLs considering protection systems in Korean power distribution system," *Superconductivity and Cryogenics*, vol. 11, no. 3, pp. 50–54, 2009.

[4] H. Lee, H. M. Kim, B. W. Lee, I. S. Oh, H.-R. Kim, O. B. Hyun, J. Sim, H. M. Chang, J. Bascuñán, and Y. Iwasa, "Conduction-cooled brass current leads for a resistive Superconducting Fault Current Limiter (SFCL) system," *IEEE Trans. Appl. Supercond.*, vol. 17, pp. 2248–2251, 2007.

[5] S. Figliola and D. E. Beasley, *Theory and Design for Mechanical Measurements*, 4th ed. Hoboken, N.J.: Wiley, 2006.

[6] W. Riley, L. Sturges, and D. Morris, *Mechanics of Materials*, 6 ed. : Wiley, 2006.